

RSC Advances



This is an *Accepted Manuscript*, which has been through the Royal Society of Chemistry peer review process and has been accepted for publication.

Accepted Manuscripts are published online shortly after acceptance, before technical editing, formatting and proof reading. Using this free service, authors can make their results available to the community, in citable form, before we publish the edited article. This *Accepted Manuscript* will be replaced by the edited, formatted and paginated article as soon as this is available.

You can find more information about *Accepted Manuscripts* in the [Information for Authors](#).

Please note that technical editing may introduce minor changes to the text and/or graphics, which may alter content. The journal's standard [Terms & Conditions](#) and the [Ethical guidelines](#) still apply. In no event shall the Royal Society of Chemistry be held responsible for any errors or omissions in this *Accepted Manuscript* or any consequences arising from the use of any information it contains.

**Effect of branching in remote substituents on light emission and stability of
chemiluminescent acridinium esters**

Anand Natrajan* and David Wen

*Siemens Healthcare Diagnostics
Advanced Technology and Pre-Development
333 Coney Street
East Walpole, MA 02032*

* Author to whom correspondence should be directed.

E-mail: anand.natrajan@siemens.com

Phone: 1-508-660-4582

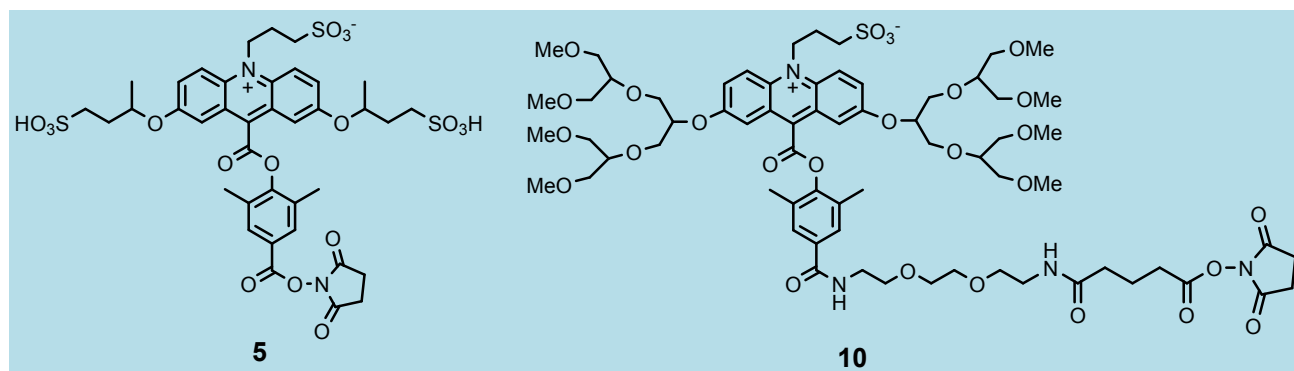
Fax: 1-508-660-4591

Abstract

Acridinium dimethylphenyl esters are widely used as chemiluminescent labels in automated immunoassays for clinical diagnostics in Siemens Healthcare Diagnostics' ADVIA Centaur[®] systems. Light emission from these labels and their conjugates is triggered with alkaline peroxide. Excited state acridone is believed to be the light emitting species that is formed from the initial peroxide adduct which subsequently undergoes a series of reactions leading to scission of the phenolic ester bond. Dioxetane and/or dioxetanone intermediates have been proposed as immediate precursors of excited state acridone.

Despite the fact that acridinium esters have been widely used as chemiluminescent labels for decades, a substantive theoretical framework to guide acridinium ester design with improved properties over the basic structure is unavailable. We have relied on a more empirical approach to devise new acridinium esters with improved stability, higher light yield, fast light emission, low non-specific binding and improved immunoassay performance. In the current study, we have investigated the effect of branching in remote alkoxy substituents attached to C-2 and C-7 of the acridinium ring on light emission and chemiluminescence stability of two acridinium esters. We selected two, high light output acridinium dimethylphenyl esters that we described previously as a basis for these studies and report the synthesis of two new C-2 and C-7 alkoxy-substituted labels, compounds **5** and **10**, with improved chemiluminescence stability and faster light emission respectively. Compound **5** exhibited better long term stability at both pH 6 and 7.4 ($\geq 10\%$) compared to its unbranched counterpart compound **11** whereas compound **10** with branched hexa(ethylene) glycol substituents exhibited > 4-fold faster light emission compared to its unbranched counterpart **12**. Both parameters are important for immunoassay performance in automated instruments.

Graphical Abstract



Keywords: acridinium dimethylphenyl esters, branched phenolic ethers, improved stability, fast light emission.

Introduction

Acridinium dimethylphenyl esters¹ (structures illustrated in Figure 1) are widely used as chemiluminescent labels in automated immunoassays for clinical diagnostics in Siemens Healthcare Diagnostics' ADVIA Centaur[®] systems. Light emission from these labels is triggered by the sequential addition of two reagents. An initial treatment with 0.1 M nitric acid containing 0.5% hydrogen peroxide converts the non-chemiluminescent water adducts of the acridinium esters, (**I** in Figure 2) that are also commonly referred to as pseudobases², to the chemiluminescent acridinium forms of the labels (**II** in Figure 2). Subsequent addition of 0.25 M sodium hydroxide ionizes the hydrogen peroxide which reacts with the acridinium ester eventually leading to excited state acridone **VI**. Dioxetane **IV** and dioxetanone **V** have been proposed as intermediates in the chemiluminescent reaction pathway of acridinium esters³. Recent theoretical studies suggest that excited state acridone **VI** is formed directly from dioxetane **III**³. Details regarding this process are not well understood although light emission is believed to result from a single electronically excited state of the acridone^{3d,e}.

The cationic surfactant cetyltrimethylammonium chloride (CTAC) is included in 0.25 M sodium hydroxide when light emission is triggered from acridinium dimethylphenyl esters and their conjugates. In the absence of CTAC, light emission from the labels and conjugates is relatively slow and can take up to a minute for complete emission. Overall light yield in the absence of CTAC is also significantly lower. Inclusion of CTAC compresses emission times of the labels to < 5 seconds and also increases overall light yield 3-4 fold^{1c,e}. These effects result from the high local concentration of hydroperoxide ions at the cationic micellar surface which accelerates their reaction with micelle-bound acridinium ester, as well as a less polar micellar medium which in turn facilitates formation of dioxetane and dioxetanone precursors of the primary emitter, excited state acridone **VI**. The observed enhancement in acridinium ester chemiluminescence (light yield) is quite sensitive to the polarity of the micellar interface^{1c}.

Although acridinium esters have been used as chemiluminescent labels for quite some time now, but for a few mechanistic studies^{3c,d,e}, a theoretical framework which can be used to predict and tailor the properties of these commercially-useful labels is not available. In its absence, we have relied on a more empirical approach and in recent publications, we have outlined studies that have proved useful to devise new acridinium ester structures with improved stability, higher light yield, fast light emission, low non-specific binding and improved immunoassay performance¹. These studies have also provided us with important insights into the chemiluminescence pathway of acridinium esters as well as some useful principles for acridinium ester design.

In a recent study^{1a,b}, we evaluated the effect of methoxy groups placed at various positions in the acridinium ring (see Figure 1 for numbering system) on light emission from the corresponding acridinium esters. Maximum light yield was observed with the placement of two methoxy groups at C-2 and C-7 of the acridinium ring. Although a 2,7-dimethoxy-substituted acridinium dimethylphenyl ester proved to be considerably less stable than an unsubstituted acridinium ester, replacement of the methoxy groups with bulkier methoxyhexa(ethylene) glycol groups surprisingly improved chemiluminescence stability without compromising the high light yield observed with the methoxy-substituted analog^{1b}. An acridinium ester label with C-2 and C-7, methoxyhexa(ethylene) glycol groups along with a hexa(ethylene) glycol linker attached to the phenol, also exhibited low non-specific binding and enhanced assay sensitivity in a sandwich assay for TSH (TSH = thyroid stimulating hormone)^{1b}. A structural variant of this label^{1a} with a simpler linker attached to the phenol to facilitate protein labeling (Figure 3, compound **12**), is currently used for measurement of the cardiac marker troponin I peptide (TnI) in the ADVIA Centaur[®] TnI-Ultra assay.

Instability of acridinium esters is generally attributed to hydrolysis of the phenolic ester bond⁴. The improved stability of compound **12** compared to the methoxy-substituted analog

clearly illustrates that structural changes in alkoxy substituents that increase their steric bulk even when located remote from the phenolic ester linkage can affect stability of acridinium esters. Because branching is expected to further increase the steric bulk of substituents, in the current study, we have investigated the effect of branching at these remote alkoxy substituents on the light emission and chemiluminescence stability of two acridinium dimethylphenyl esters (Figure 3).

Results and Discussion

Synthesis of acridinium esters and bovine serum albumin (BSA) conjugates

To investigate the effect of branching in remote C-2 and C-7 alkoxy substituents in acridinium esters on their properties, we selected two different acridinium esters **5** and **10** for synthesis (Figure 3). Compound **5** is an analog of **11**, a strongly anionic label whose synthesis we described recently^{1f}. Compound **5** contains additional branching at the phenolic ethers at C-2 and C-7. The introduction of two methyl groups in **5** represents only a small structural change in the acridinium ring compared to **11** and is not expected to significantly increase the hydrophobicity of the acridinium ester. Compound **10** is an analog of **12** with branched instead of linear hexa(ethylene) glycol groups attached to C-2 and C-7 of the acridinium ring.

The synthesis of the anionic label **5** is illustrated in Figure 4 and follows an analogous route that we described recently for compound **11**^{1f}. In the case of **11**, 2,7-dihydroxyacridine ester **1** was alkylated at the two phenolic hydroxyl groups as well as the acridine nitrogen in one step with 1,3-propane sultone^{1f}. For the O-alkylation reaction leading to compound **5**, we used 1,3-butane sultone **2** as the alkylating reagent. The sultone **2** was synthesized from the methane sulfonate (mesylate) diester of 1,2-propane diol using a literature procedure⁵. As before, the O-alkylation reaction was conducted in the ionic liquid 1-butyl-3-methylimidazolium hexafluorophosphate [BMIM][PF₆] in the presence of potassium carbonate as base. Despite the lower reactivity of **2** which entails ring opening at a secondary carbon instead of a primary

carbon in 1,3-propane sultone, nevertheless, in preparative reactions, we observed excellent conversion to the O-dialkylated product **3** when the crown ether dibenzo-18-crown-6 was included in the alkylation reaction even with only 3 equivalents of the sultone **2**. Interestingly, the lowered reactivity of **2** ensured no N-alkylation at the acridine nitrogen which is much more sterically hindered⁶ even when 15 equivalents of sultone **2** were used in the O-alkylation reaction. The sultone **2** is chiral and two sets of diastereomers are possible for the O-alkylated product **3**. HPLC analysis of the O-alkylation reaction using a high resolution column did indeed indicate the formation of a pair of diastereomers eluting close together (Figure S1, supplementary material). A small quantity of each isomer was isolated by HPLC (Figures S1a and S1b, supplementary material) and both showed very similar high field proton NMR spectra (Figures S8 and S9, supplementary material) and identical mass spectra (experimental section). Separation of the isomers was not practical for preparative purposes and therefore, they were carried forward together to the next step in an one pot reaction which entailed O-alkylation as described above followed by N-alkylation of the acridine nitrogen with 1,3-propane sultone in [BMIM][PF₆] in the presence of 2,6-di-*tert*-butylpyridine as base^{6a}. The N-sulfopropyl acridinium carboxylic acid **4** was obtained after hydrolysis of the N-sulfopropyl acridinium methyl ester and was subsequently converted to the target compound **5** using standard chemistry for N-hydroxysuccinimide (NHS) ester formation.

Synthesis of the acridinium ester **10** with branched hexa(ethylene) glycol groups at C-2 and C-7 of the acridinium ring also started with 2,7-dihydroxyacridine ester **1** as illustrated in Figure 5. Compound **6** which, is a branched isomer of methoxyhexa(ethylene) glycol, was synthesized using a literature procedure and followed a common synthetic protocol that is used for the assembly of these types of branched glycerol derivatives⁷. Thus, as described in the published procedure, reaction of epichlorohydrin with methanol afforded 1,3-dimethoxyglycerol^{8a,b} which was again treated with epichlorohydrin in the presence of base to

give compound **6^{8b}** (experimental section). Coupling of compound **6** and dihydroxyacridine ester **1** to establish the phenolic ether linkages was accomplished using the Mitsunobu reaction⁹ which gave the C-2 and C-7 di-substituted acridine ester **7**. Acridine ester **7** was then N-alkylated with 1,3-propane sultone in [BMIM][PF₆] in the presence of 2,6-di-*tert*-butylpyridine to introduce the N-sulfopropyl group. Hydrolysis of the N-sulfopropyl acridinium methyl ester intermediate gave the acridinium carboxylic acid **8**. Activation of the carboxylic acid **8** followed by condensation with a commercially available linker 2,2'-(ethylenedioxy)bis(ethylamine) gave compound **9** which was further reacted with glutaric anhydride followed by activation of the glutarate intermediate to give target **10**. Although compound **10** contains a different linker compared to compound **12**, we reasoned that the slightly longer linker in **10** would facilitate protein labeling and offset the steric hindrance caused by the bulky ether substituents at C-2 and C-7 in **10**. This proved to be true during labeling of BSA with five equivalents input of each of the various acridinium esters as can be noted in Table 1. Mass spectral analysis indicated the incorporation of 3-5 labels for the various labels using the labeling protocol described in the experimental section. HPLC chromatograms of all synthetic intermediates and final compounds of Figures 4 and 5 are shown in the supplementary section (Figures S1-S7).

Chemiluminescence measurements, stability and pseudobase formation

Light yield (specific activity) and emission times from BSA conjugates of the acridinium esters **5**, **10** and their counterparts **11** and **12** (without branching at C-2 and C-7) are listed in Table 1. The emission profiles are illustrated in Figures 6 and 7. For all the acridinium esters, we used BSA conjugates instead of the free labels to ensure complete solubility of the labels in aqueous buffer especially at high dilution that were needed for measurements in the linear range of the photomultiplier tube in the luminometer. (In our previous study we observed that micellar effects on the chemiluminescence of acridinium ester labels are very similar for the free labels as well as the conjugates of the labels^{1c,e}). The conjugates ~2 mg/mL were serially

diluted into buffer to final concentrations of approximately 0.3 nanomolar (nM) and chemiluminescence was measured using a luminometer from Berthold Technologies. Light emission from 0.01 mL samples were initiated by the sequential addition of 0.3 mL of 0.1 M nitric acid with 0.5% hydrogen peroxide (reagent 1) followed by the addition of 0.25 M sodium hydroxide (reagent 2) with and without 7 mM (5 times the critical micelle concentration¹⁰) of the cationic surfactant CTAC. Light was measured for 20 seconds integrated at 0.1 s intervals. For measurements in the absence of CTAC, light was measured for 2 minutes integrated at 0.5 s intervals. (Additional details can be found in the experimental section.) The output of the instrument is expressed as Relative Light Units (RLUs).

As can be noted from Table 1, the specific chemiluminescent activity (SCA), expressed as RLUs per mole, of the various labels are quite comparable. This is unsurprising because all four acridinium esters **5**, **10**, **11** and **12** have the same C-2 and C-7 dialkoxy-substituted motif which is the main determinant of light yield based on our earlier study^{1a,b}. Emission times, as reflected by the time needed for $\geq 95\%$ emission of total light, however showed a significant difference for the two acridinium esters **10** and **12** containing linear versus branched hexa(ethylene) glycol substituents. Acridinium ester **10** with branched hexa(ethylene) glycol groups showed much faster emission (> 4 -fold faster) compared to **12** for $\geq 95\%$ emission of total light in the presence of CTAC (Table 1). A comparison of the emission profiles of these acridinium esters in the presence of CTAC (Figure 6) and in its absence (Figure 7) showed that the differences in the emissive rates of these two compounds is an intrinsic one based on structural differences between the C-2 and C-7 alkoxy substituents. In the absence of CTAC, light emission from **10** and **12** was relatively slow (Figure 7) but **10** still showed comparatively faster emission than **12**.

On the other hand, for the two strongly anionic labels **5** and **11**, emission times were quite similar to each other both in the presence and absence of CTAC as can be noted from

Table 1 and the emission profiles in Figures 6 and 7. In this case, branching at the phenolic ethers at C-2 and C-7 had little impact on emission times. As noted for **10** and **12**, in the absence of CTAC light emission from **5** and **11** was relatively slow but was much faster in the presence of CTAC.

We next compared the chemiluminescent stability of the BSA conjugates of the acridinium esters **5**, **10**, **11** and **12** at pH 6 and 7.4 over a period of five weeks and the results are shown in Tables 2 and 3. The conjugates of the acridinium esters were diluted into phosphate buffer at pH 6 and 7.4 as described earlier and were stored at room temperature (25° C) protected from light. Chemiluminescence from 0.01 mL samples was measured periodically (five replicates) and the observed RLUs were averaged and converted to percentages. The initial observed RLUs at the first time point (day 1) was assigned a value of 100% and residual chemiluminescence as a percentage of this initial value reflects the chemiluminescence stability. (Details of the measurements can be found in the experimental section). As observed previously for an antibody conjugate^{1f}, the BSA conjugate of the anionic label **11** in the current study, was again observed to be more stable at acidic pH 6 than at pH 7.4 (Table 2). Interestingly, while branching at the phenolic ethers in the structurally analogous, strongly anionic label **5** had a minimal impact on emission kinetics, its chemiluminescence stability was observed to be better at both pH 6 and 7.4. Consistent with our previous observations for **11**, the conjugate of **5** was also observed to be more stable at pH 6 compared to pH 7.4. Stability comparison of the BSA conjugates of compounds **10** and **12** with branched and linear hexa(ethylene) glycol groups respectively, on the other hand, showed a much smaller and perhaps insignificant difference in stability between the two structures at either pH (Table 3).

Chemiluminescence instability of acridinium esters is attributed to hydrolysis of the phenolic ester with simple unsubstituted phenyl esters exhibiting poor stability⁴. This instability is alleviated considerably for acridinium dimethylphenyl esters due to steric shielding afforded by

the two methyl groups flanking the phenolic ester⁴. Another factor we have observed that impacts chemiluminescence stability of acridinium esters is the pKa of the acridinium-pseudobase transition^{1b,f}. The acridinium form **I** (Figure 1) is expected to be more susceptible to hydrolysis of the phenolic ester due to electron withdrawal from the quaternary acridinium nitrogen. Thus, acridinium esters with a higher pKa for the acridinium to pseudobase transition are expected to be less stable and this prediction appears to be generally true^{1b,f}. (At a given pH, a greater proportion of the acridinium ester is in the labile acridinium form if it has a higher pKa). In fact pseudobase-type adducts formed by the addition of various sulfhydryl-containing nucleophiles have been shown to enhance the hydrolytic stability of simple acridinium phenyl esters^{2c}.

Acridinium esters with a higher pKa for pseudobase formation are also predicted to have a less electrophilic C-9 because pseudobase formation occurs at a higher pH. Does this translate to a slower reaction with hydroperoxide ions which add at C-9 as a first step in the chemiluminescence reaction pathway of acridinium esters (Figure 2)? Our empirical observations^{1f} suggest that pKa of pseudobase formation of different acridinium esters are not necessarily correlated with observed emission kinetics. Thus, in our previous study^{1f}, we noted that acridinium esters with different pKas for pseudobase formation exhibited similar emission kinetics.

Are the observed differences in chemiluminescence stability of the acridinium esters **5** and **10** with branched C-2 and C-7 phenolic ethers versus their unbranched counterparts **11** and **12** due to a shift in the pKa for pseudobase formation to acidic pH? To answer this question, we measured the pKa of pseudobase formation (conversion of **II** to **I** in Figure 2) of the various acridinium esters using a simple pH titration method that we described previously^{1e,f} (Figures 8 and 9). Briefly, the long wavelength absorption band of the acridinium chromophore is measured as a function of pH. Pseudobase formation disrupts the conjugation of the acridinium

ring and results in a loss of the long wavelength absorption band. Typically, a sharp transition over a narrow range of pH is noted for the acridinium to pseudobase formation as illustrated in Figures 8 and 9. As can be noted from Figure 8, introduction of branching at the phenolic ethers in **5** induced a small shift in the pKa (~ 0.5 unit) for pseudobase formation to acidic pH when compared to **11** which would be more conducive to the improved chemiluminescence stability of **5** observed in Table 2. However, stability differences between **10** and **12** were minimal as noted in Table 3 yet **10** with branched hexa(ethylene) glycol groups also showed a small and equivalent shift in pKa for pseudobase formation to acidic pH when compared to its linear counterpart **12**. The reason why branching at a remote substituent in an acridinium ester affects its pKa is unclear but may reflect relief of steric crowding caused by a flat acridinium ring and branched functional groups attached in close proximity to the acridinium ring system. Pseudobase formation presumably relieves this steric crowding because the acridine ring in the pseudobase is no longer flat. Observed differences in chemiluminescence stability of the various acridinium esters, **5** versus **11** and **10** versus **12** however cannot be attributed entirely to shifts in the pKa for pseudobase formation to acidic pH at least for **10** and **12**. These remote substituents must also affect formation and/or decomposition of the sterically-crowded tetrahedral intermediates involved in phenolic ester hydrolysis.

Finally, what explains the difference in emission kinetics between **10** and **12**? If addition of hydroperoxide ions at C-9 is equally facile for **10** and **12** (Figure 2), then the increase in emissive rates for **10** must result from faster decomposition of the dioxetane intermediate. If the steric bulk of remote C-2 and C-7 functional groups can affect stability of the phenolic ester as we observed previously^{1b} and in the current study, it is reasonable to expect that the steric bulk of remote substituents may also affect the stability and decomposition of the dioxetane intermediate **III** (Figure 2). The fast light emission observed for **10** compared to **12** suggests that the branched hexa(ethylene) glycol group imposes greater steric constraints than the linear

hexa(ethylene) glycol substituent which can adopt an extended conformation in aqueous solution.

Conclusions

In the current study we have described the syntheses of two new acridinium esters **5** and **10** based on the high light yielding, C-2 and C-7 dialkoxy-substituted structural motif. The new structures contain additional branching at these alkoxy groups which were observed to impact both chemiluminescence stability and emission kinetics despite being located remote from the reaction centers affecting these two parameters. From a practical point of view, both new structures **5** and **10** are improvements over their corresponding predecessors **11** and **12**. In the case of the strongly anionic label **5**, better chemiluminescence stability was observed compared to **11** which is useful for reagent stability. In the case of **10**, the improvement in chemiluminescence stability was not significant compared to **12** but the new label showed much faster light emission which is another useful feature in automated immunoassays for fast throughput because of reduced cycle times needed for each assay.

References

1. (a) A. Natrajan, Q. Jiang, D. Sharpe and J. Costello, *US Pat.*, 7,309,615, 2007; (b) A. Natrajan, D. Sharpe, J. Costello and Q. Jiang, *Anal. Biochem.*, 2010, **406**, 204-213; (c) A. Natrajan, D. Sharpe and D. Wen, *Org. Biomol. Chem.*, **2011**, 9, 5092-5103; (d) A. Natrajan, D. Sharpe and D. Wen, *Org. Biomol. Chem.*, 2012, **10**, 1883-1895; (e) A. Natrajan, D. Sharpe and D. Wen, *Org. Biomol. Chem.*, 2012, **10**, 3432-3447; (f) A. Natrajan and D. Sharpe, *Org. Biomol. Chem.*, 2013, **11**, 1026-1039.
2. (a) I. Weeks, I. Behesti, F. McCapra, A.K. Campbell and J.S. Woodhead, *Clin. Chem.*, 1983, **29/8**, 1474-1479; (b) J.W. Bunting, V.S.F. Chew, S.B. Abhyankar and Y. Goda, *Can. J. Chem.*, 1984, **62**, 351-354; (c) P.W. Hammond, W.A. Wiese, A.A. Waldrop III, N.C. Nelson and L.J. Arnold Jr, *J. Bioluminescence and Chemiluminescence*, 1991, **6**, 35-43.
3. (a) F. McCapra, *Acc. Chem. Res.*, 1976, **9/6**, 201-208; (b) F. McCapra, D. Watmore, F. Sumun, A. Patel, I. Beheshti, K. Ramakrishnan and J. Branson, *J. Bioluminescence and Chemiluminescence*, 1989, **4**, 51-58; (c) J. Rak, P. Skurski and J. Błażejowski, *J. Org. Chem.*, 1999, **64**, 3002-3008; (d) K. Krzymiński, A.D. Roshal, B. Zadykowicz, A. Białk-Bielińska and A. Sieradzan, *J. Phys. Chem. A*, 2010, **114**, 10550-10562; (e) K. Krzymiński, A. Ozóg, P. Malecha, A.D. Roshal, A. Wróblewska, B. Zadykowicz, and J. Błażejowski, *J. Org. Chem.*, 2011, **76**, 1072-1085.
4. S.-J. Law, T. Miller, U. Piran, C. Klukas, S. Chang and J. Unger, *J. Bioluminescence and Chemiluminescence*, 1989, **4**, 88-98.
5. T. Durst and K.-C. Tin, *Can. J. Chem.*, 1970, **48**, 845-851.
6. (a) A. Natrajan and D. Wen, *Green Chem.*, 2011, **13**, 913-921; (b) A. Natrajan and D. Wen, *Green. Chem. Lett. Rev.*, 2013, **3**, 237-248.
7. S. Cassel, C. Debaig, T. Benvegny, P. Chaimbault, M. Lafosse, D. Plusquellec and P. Rollin, *Eur. J. Org. Chem.*, 2001, 875-896.

8. (a) K.-T. Kang, S. Kue Lee, C. Won Park, S. Hui Cho, J. Gun Lee, S.-K. Choi and Y. Bae Kim, *Bull. Korean. Chem. Soc.*, 2006, **27**, 1364-1370; (b) T. Ishigaki, H. Fukuda, M. Yamanaka and K. Aoi, JP2007063175 A.
9. (a) O. Mitsunobu, *Synthesis*, 1981, **1**, 1-28; (b) D.L. Hughes, *Organic Reactions*; Wiley : New York, 1992, **42**, 335-656.
10. (a) L Sepúlveda and J. Cortés, *J. Phys. Chem.*, 1985, **89**, 5322-5324; (b) R. Bacaloglu, C.A. Bunton and F. Ortega, *J. Phys. Chem.* 1989, **93**, 1497-1502.

Experimental

General

Chemicals were purchased from Sigma-Aldrich (Milwaukee, Wisconsin, USA) unless indicated otherwise. The ionic liquid [BMIM][PF₆] was dried under high vacuum over P₂O₅ prior to use.

All final acridinium esters and intermediates were analyzed and/or purified by HPLC using a Beckman-Coulter HPLC system. Flash chromatography was performed using an 'Autoflash' system from TELEDYNE ISCO. MALDI-TOF (Matrix-Assisted Laser Desorption Ionization-Time of Flight) mass spectroscopy was performed using a VOYAGER DE Biospectrometry Workstation from ABI. This is a bench top instrument operating in the linear mode with a 1.2 meter ion path length, flight tube. Spectra were acquired in positive ion mode. For small molecules, α -cyano-4-hydroxycinnamic acid was used as the matrix and spectra were acquired with an accelerating voltage of 20,000 volts and a delay time of 100 nsec. For protein conjugates, sinapinic acid was used as the matrix and spectra were acquired with an accelerating voltage of 25,000 volts and a delay time of 85 nsec.

For HRMS (High Resolution Mass Spectra), samples were dissolved in HPLC-grade methanol and analyzed by direct-flow injection (injection volume = 5 μ L) ElectroSpray Ionization (ESI) on a Waters Qtof API US instrument in the positive ion mode. Optimized conditions were as follows: Capillary = 3000 kV, Cone = 35, Source Temperature = 120°C, Desolvation Temperature = 350°C. NMR spectra were recorded on a Varian 500 MHz spectrometer. IR spectra of neat samples were recorded on a Bruker TENSOR37 FT-IR spectrometer, ATR mode on ZnSe crystal. UV-Visible spectra were recorded on a Beckman DU 7500 spectrophotometer. Chemiluminescence measurements were carried out using a Berthold Technologies' AutoLumat Plus LB 953 luminometer.

1. *Synthesis of acridinium esters (Figures 4 and 5, and Figures S1-S7 supplementary section)*

Compound 3

A mixture of compound **1** (10 mg, 0.024 mmole), potassium carbonate (10 mg, 0.072 mmole), dibenzo-18-crown-6 (26 mg, 0.072 mmole) and 1,3-butane sultone **2** (49 mg, 0.359 mmole) in 1-butyl-3-methylimidazolium hexafluorophosphate [BMIMPF₆] (0.5 mL) was heated at 155°C for 2 hours. The reaction was diluted with ethyl acetate (5 mL) and applied to a silica column equilibrated with ethyl acetate. The column was first eluted with ethyl acetate (525 mL) to elute unreacted starting material and dibenzo-18-crown-6 followed by 40% methanol in ethyl (500 mL) to elute product. The product fractions were combined and concentrated under reduced pressure. The product was analyzed by analytical HPLC using a Phenomenex, Kinetex C₁₈, 50 x 4.6 mm, 2.6 micron column with a 10 minute gradient of 10 → 90% MeCN/water (each with 0.05% trifluoroacetic acid, TFA) which showed two peaks at 4.6 and 4.8 minutes. These two compounds were purified by preparative HPLC using a Phenomenex, Luna C₁₈, 250 x 30 mm column and a 40 minute gradient of 5 → 40% MeCN/water (each with 0.05% TFA). The two diastereomers were isolated separately, the HPLC fractions frozen at -80°C and lyophilized to dryness. Combined yield = 15.8 mg (96%). Diastereomer eluting at 4.6 minutes: δ_{H} (500 MHz, CF₃COOD) 1.49 (d, 6H, $J = 5.9$), 2.42 (m, 4H), 2.49 (s, 6H), 3.49 (br s, 4H), 4.05 (s, 3H), 5.02 (br s, 2H), 7.85 (br s, 2H), 7.96 (d, 2H, $J = 9.6$), 7.97 (s, 2H), 8.26 (d, 2H, $J = 9.4$); MALDI-TOF MS m/z 690.6 (M+H)⁺; HRMS m/z 690.1675 (M+H)⁺ (690.1679 calculated). Diastereomer eluting at 4.8 minutes: δ_{H} (500 MHz, CF₃COOD) 1.50 (d, 6H, $J = 5.9$), 2.42 (m, 4H), 2.50 (s, 6H), 3.49 (br s, 4H), 4.05 (s, 3H), 5.02 (br s, 2H), 7.85 (s, 2H), 7.95 (d, 2H, $J = 9.6$), 7.96 (br d, 2H), 8.26 (d, 2H, $J = 9.5$); MALDI-TOF MS m/z 690.5 (M+H)⁺; HRMS m/z 690.1671 (M+H)⁺ (690.1679 calculated).

Compound 4

A mixture of compound **1** (56 mg, 0.134 mmole), potassium carbonate (46 mg, 0.335 mmole), dibenzo-18-crown-6 (121 mg, 0.335 mmole) and 1,3-butane sultone **2** (54.8 mg, 0.402

mmole) in 1-butyl-3-methylimidazolium hexafluorophosphate (2 mL) was heated at 120°C for 2 hours. The reaction was cooled to room temperature and a small portion of the reaction mixture was analyzed by HPLC as described above which showed complete conversion to **3**. To this reaction mixture, 2,6-di-*tert*-butylpyridine (0.45 mL, 2.012 mmole) and 1,3-propane sultone (279 mg, 2.281 mmole) were added and the reaction was heated at 155°C for 16 hours. The reaction was cooled to room temperature and a small portion of the reaction mixture was analyzed by HPLC which showed 62% conversion to the N-sulfopropyl acridinium ester. The reaction mixture was partitioned between 2 N HCl solution (20 mL) and ethyl acetate (30 mL). The aqueous layer was separated and washed with another portion of ethyl acetate (30 mL). The aqueous layer was then refluxed for 4 hours and analyzed by HPLC which showed complete hydrolysis to **4**. The crude product was purified by preparative HPLC using a Phenomenex, Luna C₁₈, 250 x 30 mm column and a 40 minute gradient of 5 → 40% MeCN/water (each with 0.05% TFA). The product **4** (containing two diastereomers) fractions were collected and frozen at -80°C and lyophilized to dryness. Yield = 39.4 mg (37%). $\nu_{\max}/\text{cm}^{-1}$ 3364 (OH), 1748 and 1712 (CO), 1613, 1468, 1223, 1149; δ_{H} (500 MHz, CF₃COOD) 1.60 (d, 6H, J = 5.9), 2.53 (m, 4H), 2.63 (s, 6H), 2.97 (t, 2H, J = 6.3), 3.62 (m, 4H), 3.87 (t, 2H, J = 6.2), 5.11 (t, 2H, J = 6.2), 5.86 (t, 2H, J = 8.9), 7.95 (d, 2H, J = 2.7), 8.14 (s, 2H), 8.19 (dd, 2H, J = 9.9, 2.6), 8.87 (d, 2H, J = 10.0); MALDI-TOF MS m/z 798.2 (M+H)⁺; HRMS m/z 798.1539 (M+H)⁺ (798.1560 calculated).

Compound 5

A solution of compound **4** (23 mg, 0.028 mmole) in DMF (2 mL) was treated with diisopropylethylamine (0.025 mL, 0.142 mmole) and N,N,N',N'-tetramethyl-O-(N-succinimidyl)uronium tetrafluoroborate (TSTU, 13 mg, 0.042 mmole). The reaction was stirred at room temperature for 1 hour. HPLC analysis of the reaction mixture showed complete conversion to its NHS ester **5**. The product was purified by preparative HPLC using a

Phenomenex, Luna C₁₈, 250 x 30 mm column and a 40 minute gradient of 10 → 40% MeCN/water (each with 0.05% TFA). The product fractions containing **5** (containing two diastereomers) were frozen at -80°C and lyophilized to dryness. Yield = 9.4 mg (37%). $\nu_{\max}/\text{cm}^{-1}$ 1742 and 1686 (CO), 1469, 12081137; δ_{H} (500 MHz, CF₃COOD) 1.50 (d, 6H, $J = 6.0$), 2.43 (m, 4 H), 2.53 (s, 6H), 2.87 (m, 2H), 3.12 (s, 4H), 3.54 (m, 4H), 3.77 (t, 2H, $J = 6.7$), 4.98 (t, 2H, $J = 6.5$), 5.77 (m, 2H), 7.84 (d, 2H, $J = 2.7$), 8.05 (s, 2 H), 8.09 (dd, 2H, $J = 9.9, 2.6$), 8.77 (d, 2H, $J = 10.0$); MALDI-TOF MS m/z 895.1 (M+H)⁺; HRMS m/z 895.1735 (M+H)⁺ (895.1724 calculated).

Compound 6

1,3-Dimethoxy-2-propanol was synthesized as described in the literature⁸. Crude 1,3-dimethoxy-2-propanol (12.9 g, 0.108 mole) and potassium hydroxide (4.83 g, 0.08 mole) was stirred at 80° C under a nitrogen atmosphere until all the potassium hydroxide dissolved. Epichlorohydrin (1.85 g, 0.02 mole) was then added drop wise and the reaction was heated at 80° C under a nitrogen atmosphere for 16 hours. The reaction was then cooled to room temperature and quenched with acetic acid (10 mL). The resulting suspension was poured into ethyl acetate (150 mL) and after thorough mixing it was filtered to remove the precipitated solids. The ethyl acetate extract was concentrated under reduced pressure to give a light brown oil (8.06 g) which was purified by flash chromatography using 70% hexanes, 25% ethyl acetate, 5% methanol. Product fractions ($R_f = 0.2$) were combined and concentrated under reduced pressure to give a light yellow oil. Yield = 2.46 g (42%). $\nu_{\max}/\text{cm}^{-1}$ 3454 (OH), 1456, 1111; δ_{H} (500 MHz, CDCl₃) 3.36 (s, 12H), 3.39 – 3.50 (m, 8H), 3.59 (d, 1H, $J = 6.5$), 3.61 (d, 1H, $J = 6.5$), 3.64 – 3.71 (m, 4H), 3.74 (d, 1H, $J = 4.0$), 3.93 (m, 1H); MALDI-TOF MS m/z 319.2 (M+Na)⁺; HRMS m/z 319.1725 (M+Na)⁺ (319.1733 calculated).

Compound 7

A solution of compound **1** (50 mg, 0.12 mmole), compound **6** (140 mg, 0.48 mmole) and triphenylphosphine (TPP, 126 mg, 0.48 mmole) was treated with triethylamine (TEA, 0.098 mL,

0.72 mmole) and the solution was cooled in an ice bath. After 10-15 minutes, diisopropylazodicarboxylate (DIAD, 0.094 mL, 0.48 mmole) was added, the reaction was stirred briefly in the ice bath (10 minutes) and was then warmed to room temperature and stirred under a nitrogen atmosphere. After 3 hours, a small portion of the reaction was analyzed by HPLC using a Phenomenex, C₁₈ 3.9 mm x 30 cm column and a 30 minute gradient of 10 → 100% MeCN/water (each with 0.05% trifluoroacetic acid) at a flow rate of 1.0 mL/minute and UV detection at 260 nm. Product was observed eluting at 25.2 minutes and was the major component. The reaction mixture was then diluted with ethyl acetate (50 mL) and washed with 1N HCl (25 mL) followed by de-ionized water several times. The ethyl acetate extract was then dried over anhydrous magnesium sulfate and concentrated under reduced pressure. The crude product was purified by flash chromatography on silica using ethyl acetate as eluent. Yield = 59.4 mg (51%). $\nu_{\max}/\text{cm}^{-1}$ 1724 (CO), 1457, 1438, 1230, 1118; δ_{H} (500 MHz, CDCl₃) 2.46 (s, 6H), 3.25 (s, 12H), 3.29 (s, 12 H), 3.34 – 3.46 (m, 16H), 3.58 – 3.63 (m, 4H), 3.86 – 3.94 (m, 4H), 3.95 (s, 3H), 3.94 – 3.98 (m, 4H), 4.73 (p, 2H, $J = 5.1$), 7.54 (dd, 2H, $J = 9.4, 2.6$), 7.72 (d, 2H, $J = 2.6$), 7.90 (s, 2H), 8.15 (d, 2H, $J = 9.4$); MALDI-TOF MS m/z 974.8 (M+H)⁺; HRMS m/z 974.4758 (M+H)⁺ (974.4749 calculated).

Compound 8

A mixture of compound **7** (59 mg, 0.061 mmole), distilled 1,3-propane sultone (0.110 g, 0.91 mmole) and 2,6-di-*tert*-butylpyridine (0.067 mL, 0.31 mmole) in 1-butyl-3-methylimidazolium hexafluorophosphate (1 mL) was heated at 150°C for 24 hours. The reaction was cooled at room temperature and a small portion of the reaction mixture was analyzed by HPLC as described above. Approximately 65% conversion to the N-sulfopropyl acridinium ester was noted eluting at 20 minutes in a clean reaction. The reaction was diluted with ethyl acetate (5 mL) and applied to a silica column equilibrated with ethyl acetate. The column was first eluted with ethyl acetate (500 mL) to elute unreacted starting material and base followed by 1:1 ethyl acetate : methanol (500 mL) to elute product. The product fractions were combined and

concentrated under reduced pressure. The N-sulfopropyl acridinium methyl ester was refluxed in 1N HCl (10 mL) for 2 hours. The reaction was then cooled to room temperature and analyzed by HPLC which showed clean formation of product **8** eluting at 17.8 minutes. The product was purified by preparative HPLC using an YMC, C₁₈, 30 x 250 mm column and the same gradient used for analytical analysis. Product fractions containing **8** were combined and concentrated under reduced pressure. Yield = 34 mg (51%). $\nu_{\max}/\text{cm}^{-1}$ 1752 and 1714 (CO), 1613, 1468, 1148; δ_{H} (500 MHz, CF₃COOD) 2.54 (s, 6H), 2.88 (m, 2 H), 3.46 (s, 12H), 3.50 (s, 12H), 3.72 (m, 16H), 3.79 (m, 2H), 3.93 (m, 4H), 4.06 (m, 8H), 4.98 (p, 2H, $J = 4.8$), 5.78 (m, 2H), 7.98 (d, 2H, $J = 2.6$), 8.06 (s, 2H), 8.16 (dd, 2H, $J = 10.1, 2.6$), 8.81 (d, 2H, $J = 10.0$); MALDI-TOF MS m/z 1082.4 (M+H)⁺; HRMS m/z 1082.4674 (M+H)⁺ (1082.4631 calculated).

Compound 9

A solution of compound **8** (34 mg, 0.031 mmole) in DMF (2 mL) was treated with diisopropylethylamine (0.0082 mL, 0.047 mmole) and N,N,N',N'-tetramethyl-O-(N-succinimidyl)uronium tetrafluoroborate (TSTU, 14.2 mg, 0.047 mmole). The reaction was stirred at room temperature. After 30 minutes HPLC analysis as described above indicated complete conversion to the N-hydroxysuccinimide ester eluting at 19.3 min. This solution was added drop wise to a stirred solution of 2,2'-(ethylenedioxy)bis(ethylamine) (0.047 mL, 10 equivalents) dissolved in DMF (2 mL). The resulting solution was stirred at room temperature. After 30 minutes, HPLC analysis indicated complete conversion to product **9** eluting at 14.6 minutes. The product was purified by preparative HPLC as described above. HPLC fractions were concentrated under reduced pressure. Yield = 28.4 mg (74%). $\nu_{\max}/\text{cm}^{-1}$ 1751 and 1689 (CO), 1613, 1468, 1223, 1163, 1117; δ_{H} (500 MHz, CD₃COOD) 2.71 (s, 6H), 2.88 (m, 2H), 3.37 (s, 12H), 3.43 (s, 12H), 3.53 – 3.64 (m, 18H), 3.80 – 3.95 (m, 14H), 4.05 – 4.17 (m, 8H), 5.07 (m, 2H), 5.95 (m, 2H), 7.97 (s, 2H), 8.04 (d, 2H, $J = 2.7$), 8.36 (dd, 2 H, $J = 10.0, 2.7$), 9.08 (d, 2H, J

= 10.1); MALDI-TOF MS m/z 1212.9 (M+H)⁺; HRMS m/z 1212.5729 (M+H)⁺ (1212.5737 calculated).

Compound 10

A solution of compound **9** (15.4 mg, 0.013 mmole) in methanol (2 mL) was treated with diisopropylethylamine (0.011 mL, 5 equivalents) and glutaric anhydride (0.0072 mg, 5 equivalents). The reaction was stirred at room temperature. After 30 minutes, HPLC analysis as described above showed complete conversion to the glutarate derivative eluting at 16.2 minutes. The reaction mixture was concentrated under reduced pressure. The residue was suspended in anhydrous toluene (5 mL) and was evaporated to dryness. The crude glutarate derivative was dissolved in DMF (2 mL) and treated with diisopropylethylamine (0.022 mL, 10 equivalents) and TSTU (38 mg, 10 equivalents). The reaction was stirred at room temperature. After 15 minutes, HPLC analysis of the reaction mixture showed the NHS ester **10** as the major product (~80% conversion) eluting at 17.2 minutes. The product was purified by preparative HPLC as described earlier. The HPLC fractions containing **10** were frozen at -80°C and lyophilized to dryness. Yield = 12.3 mg (67%). $\nu_{\max}/\text{cm}^{-1}$ 1815, 1781, 1741 and 1689 (CO), 1613, 1468, 1204, 1136; δ_{H} (500 MHz, CD₃COOD) 2.53 (t, 2H, $J = 7.4$), 2.71 (s, 6H), 2.80 (t, 2H, $J = 7.2$), 2.84 – 2.91 (m, 2H), 2.98 (s, 4H), 3.37 (s, 12H), 3.42 (s, 12H), 3.53 – 3.64 (m, 18H), 3.76 (t, 2H, $J = 5.4$), 3.79 – 3.93 (m, 14H), 4.05 – 4.17 (m, 8H), 5.07 (m, 2 H), 5.95 (m, 2H), 7.97 (s, 2H), 8.04 (d, 2H, $J = 2.6$), 8.36 (dd, 2H, $J = 10.0, 2.7$), 9.08 (d, 2H, $J = 10.1$); MALDI-TOF MS m/z 1423.6 (M+H)⁺; HRMS m/z 1423.6245 (M+H)⁺ (1423.6217 calculated).

2. Synthesis of BSA conjugates of acridinium esters (Table 1)

BSA (1 mg, 15 nanomoles, 0.2 mL of a 5 mg/mL solution) was diluted with 0.2 mL of 0.1 M sodium carbonate, pH 9. The protein solutions, in separate labeling reactions, were treated with five equivalents of various acridinium esters of Figure 3. The acridinium esters were dissolved in dimethyl sulfoxide to give 2 mg/mL solutions. For labeling with the various

acridinium esters, 5 equivalents of the DMSO solution was added. The reactions were stirred at room temperature for 2 hours. The reactions were then diluted with 0.5 mL de-ionized water and transferred to 4 mL Amicon filters from Millipore (MW 30,000 cutoff). The labeling reactions in the filters were further diluted with 3 mL de-ionized water. The solutions were concentrated to ~ 0.1 mL by centrifugation at 7000 G for 10 minutes. This dilution and concentration process was repeated three more times. The final conjugate solutions were transferred to vials and the solutions were frozen and lyophilized. The lyophilized conjugates were dissolved in 0.5 mL of de-ionized water. The conjugates were analyzed by MALDI-TOF mass spectrometry to measure acridinium ester incorporation. This entailed measuring the molecular weight of the unlabeled protein and the labeled protein. The acridinium ester label contributed to the observed difference in mass between these two measurements. By knowing the molecular weight of the specific acridinium ester label, the extent of label incorporation for that specific acridinium ester could thus be calculated (Table 1).

3. Chemiluminescence measurements (Table 1, Figures 6 and 7)

Chemiluminescence of BSA conjugates of acridinium esters (Figure 3) was measured on an Autolumat LB953 Plus luminometer from Berthold Technologies. The conjugates, 2 mg/mL, were serially diluted 10^5 -fold for chemiluminescence measurements in an aqueous buffer of 10 mM disodium hydrogen phosphate, 0.15 M NaCl, 8 mM sodium azide and 0.015 mM bovine serum albumin (BSA), pH = 8.0. Samples of 0.010 mL volumes of each diluted acridinium ester were dispensed into the bottom of cuvettes. Cuvettes were placed into the primed LB953 and the chemiluminescence reaction was initiated with the sequential addition of 0.3 mL of reagent 1, a solution of 0.5% hydrogen peroxide in 0.1 M nitric acid followed by an almost instantaneous (< 1 second delay) addition of 0.3 mL of reagent 2, a solution of 0.25 M sodium hydroxide with or without surfactant. For measurements with CTAC, 7 mM of this cationic surfactant was included in reagent 2. In all measurements, the final pH of the chemiluminescence reaction was basic (0.15 M NaOH).

Each chemiluminescence flash curve was measured in 200 intervals of 0.1 second (20 seconds total time in the presence of CTAC or 240 intervals of 0.5 seconds (2 minutes total time), in the absence of CTAC from the point of chemiluminescence initiation with the addition of 0.25 M NaOH. Each chemiluminescence reaction was carried out a minimum of three times, averaged and converted to a percentage of the chemiluminescence accumulated up to each time interval. The output from the luminometer instrument was expressed as RLU (Relative Light Unit).

4. Measurement of chemiluminescence stability (Tables 2 and 3)

The acridinium ester labeled BSA conjugates were diluted to a concentration of 0.2 nM in a buffer of in an aqueous buffer of 10 mM phosphate, 0.15 M NaCl, 8 mM sodium azide and 0.015 mM bovine serum albumin (BSA), pH = 6.0 or 7.4. Two milliliter volumes of the diluted conjugates were sealed in glass vials and incubated at 25°C for five weeks protected from light. Chemiluminescence of 0.01 mL samples (five replicates) of the diluted conjugates was periodically measured as a function of time. Chemiluminescence was measured on a Berthold Technologies' AutoLumat Plus LB953 luminometer. The averaged results were calculated as residual chemiluminescence percentages with respect to values determined at day 1.

5. UV-Visible spectrophotometric measurements (Figures 8 and 9)

UV-Visible spectrophotometry of acridinium esters **5**, **10**, **11** and **12** for determination of the pKa of acridinium to pseudobase transition was carried out by dissolving the HPLC-purified acridinium esters in DMSO (~1 mg/mL). These solutions were further diluted 20-fold into 0.2 M phosphate or borate buffer at pH 2.0, 3.0, 4.0, 5.0, 6.0, 7.0, 8.0, 9.0 and 10.0 (pH 10 was 0.2 M borate buffer). The diluted acridinium ester solutions were allowed to stand for several hours at room temperature and then UV-Visible spectra were recorded from 220-500 nm. The absorption intensity of the long wavelength acridinium absorption band at ~ 410 nm was measured as a function of pH. A plot of this data is shown in Figures 8 and 9.

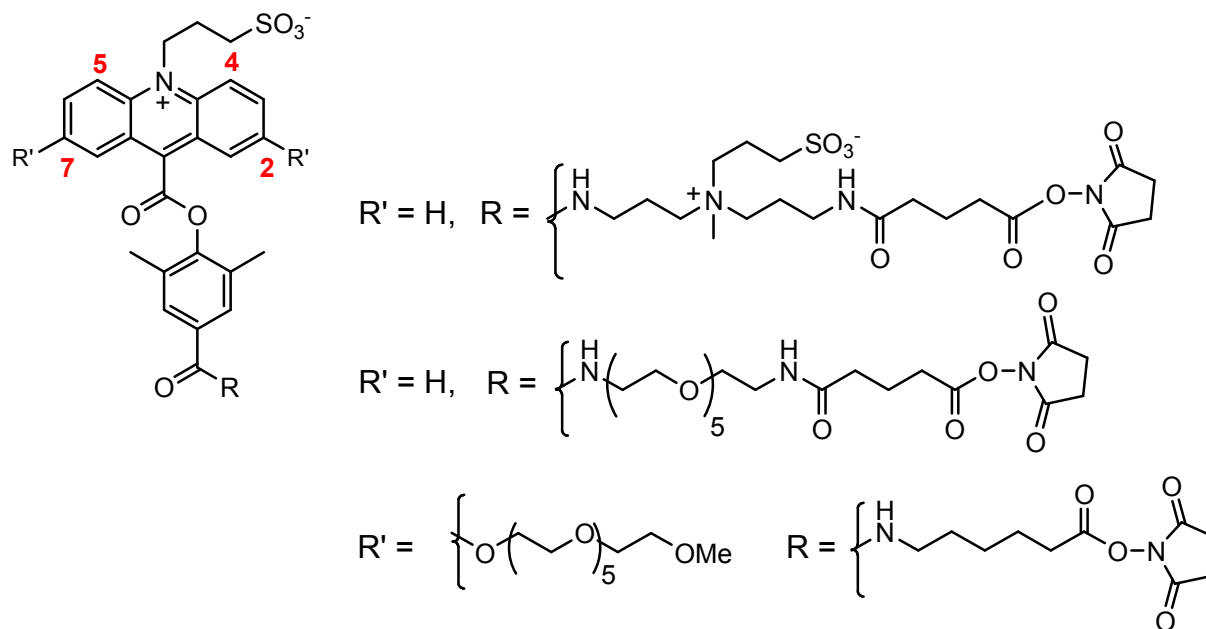


Figure 1. Structures of chemiluminescent acridinium dimethylphenyl ester labels¹ that are used in automated immunoassays in Siemens Healthcare Diagnostics' ADVIA Centaur[®] systems.

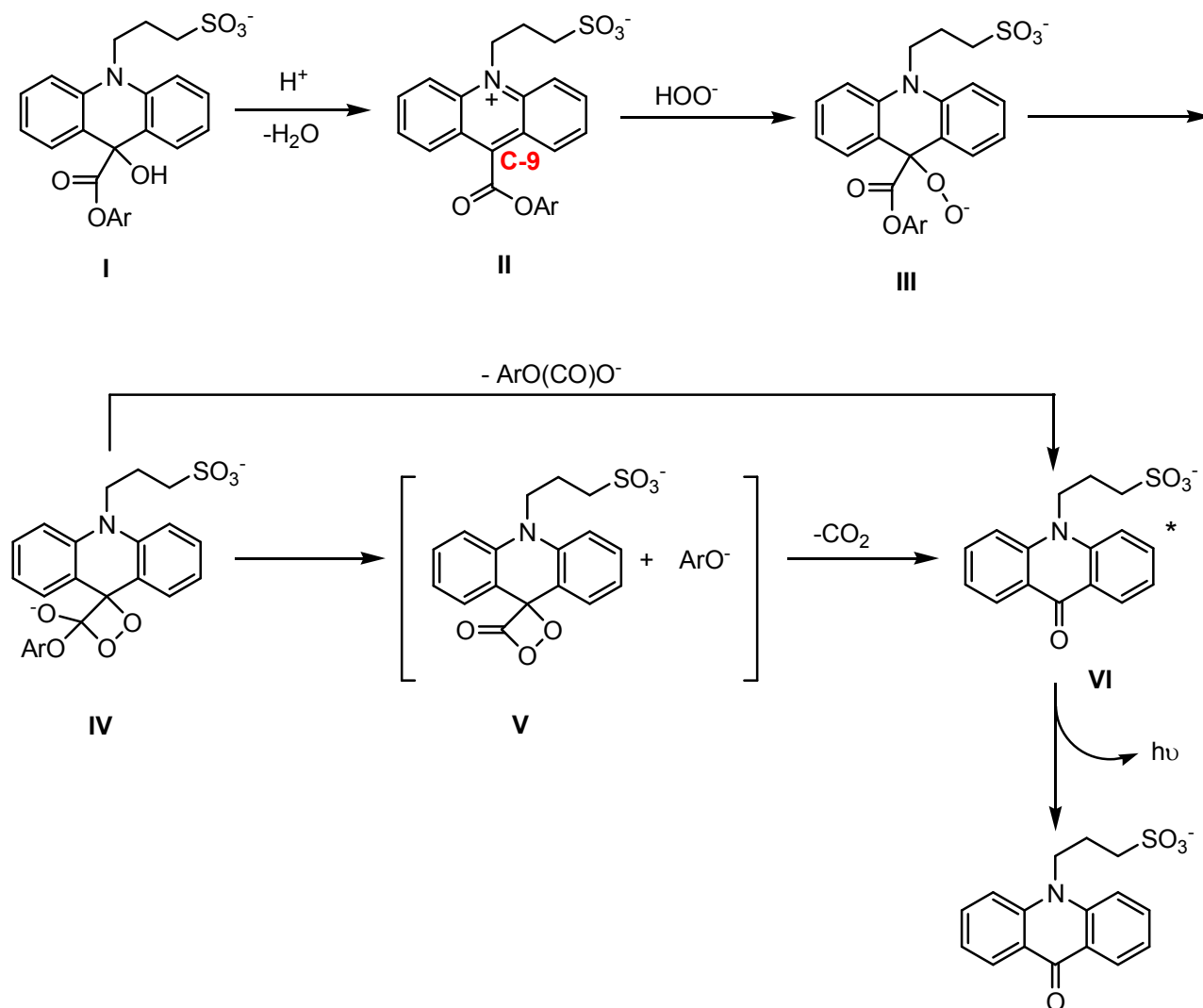


Figure 2. Simplified reaction pathway of chemiluminescence from N-sulfopropyl acridinium esters. In the ADVIA Centaur[®] system, light emission is triggered by the sequential addition of 0.1 M nitric acid followed by 0.25 M sodium hydroxide containing the cationic surfactant cetyltrimethylammonium chloride (CTAC). Acid treatment converts the water adduct **I** to the acridinium ester **II** which then reacts with alkaline peroxide ultimately resulting in excited state acridone **VI**. Dioxetane **IV** and/or dioxetanone **V** are proposed reaction intermediates. CTAC compresses emission times and increases light yield.

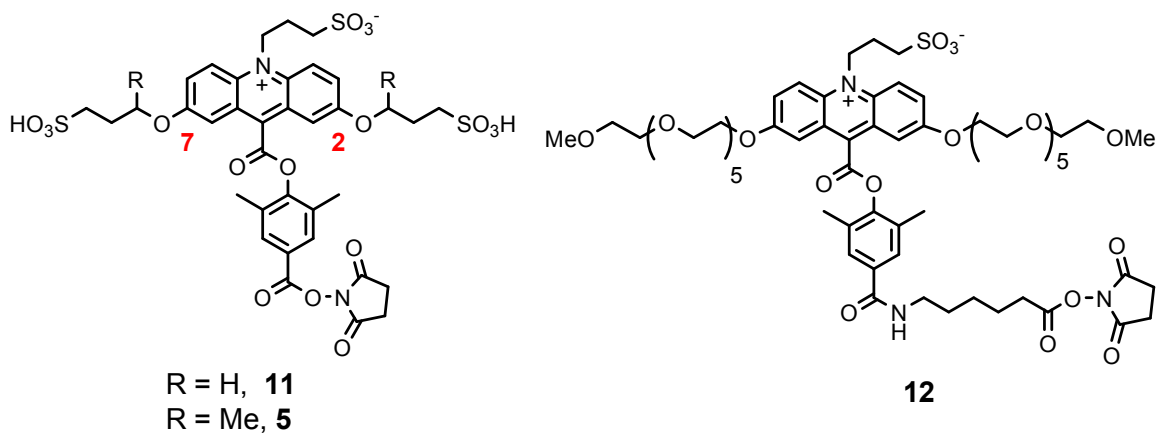


Figure 3. Structures of C-2 and C-7 dialkoxy-substituted acridinium dimethylphenyl esters. Compound **11**^{1f} is a strongly anionic N-sulfopropyl acridinium ester with two additional sulfonates appended to C-2 and C-7 of the acridinium ring. Compound **12**^{1a} is also an N-sulfopropylacridinium ester with two methoxy hexa(ethylene) glycol groups attached to C-2 and C-7 of the acridinium ring. Compounds **5** and **10** are acridinium esters synthesized in the current study. Compound **5** is an analog of **11** with additional branching at the phenolic ethers at C-2 and C-7. Compound **10** is an analog of **12** with branched hexa(ethylene) glycol groups attached to C-2 and C-7 of the acridinium ring.

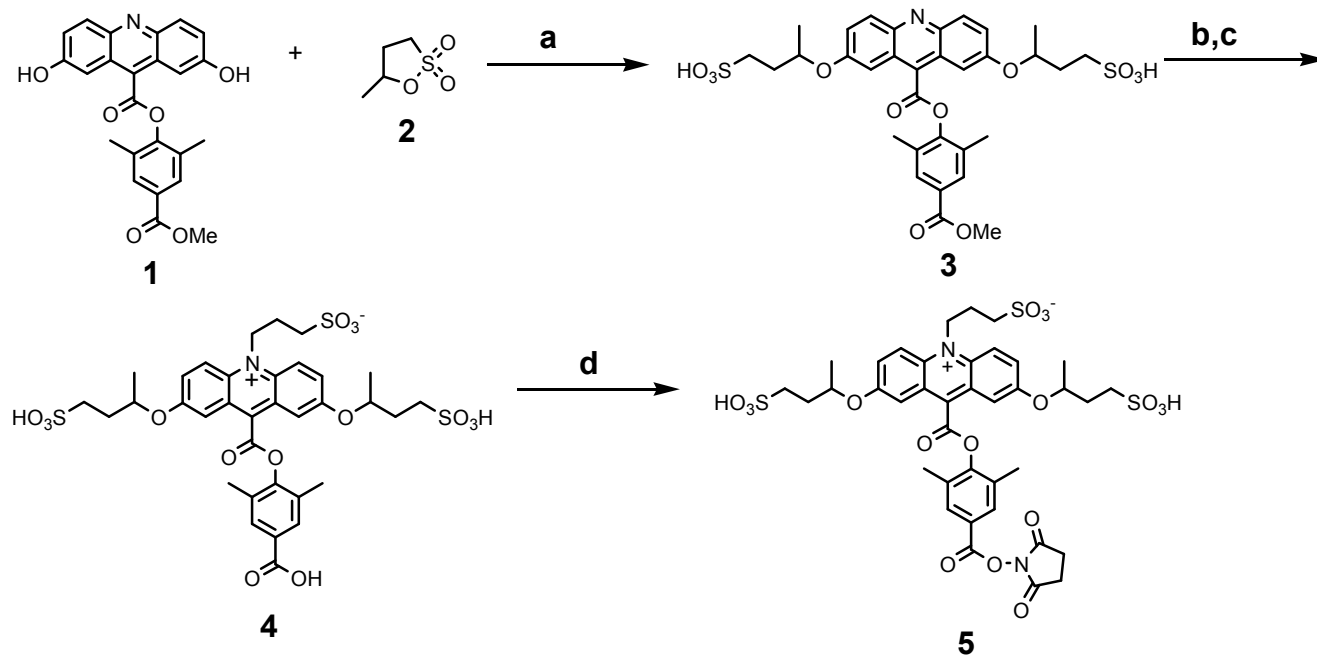


Figure 4. Synthetic scheme for compound **5**. Reagents : (a) dibenzo-18-crown-6, potassium carbonate, [BMIM][PF₆]; (b) 1,3-propane sultone, 2,6-di-*tert*-butylpyridine, [BMIM][PF₆]; (c) 2M HCl; (d) N,N,N',N'-tetramethyl-O-(N-succinimidyl)uronium tetrafluoroborate (TSTU), diisopropylethylamine (DIPEA), DMF.

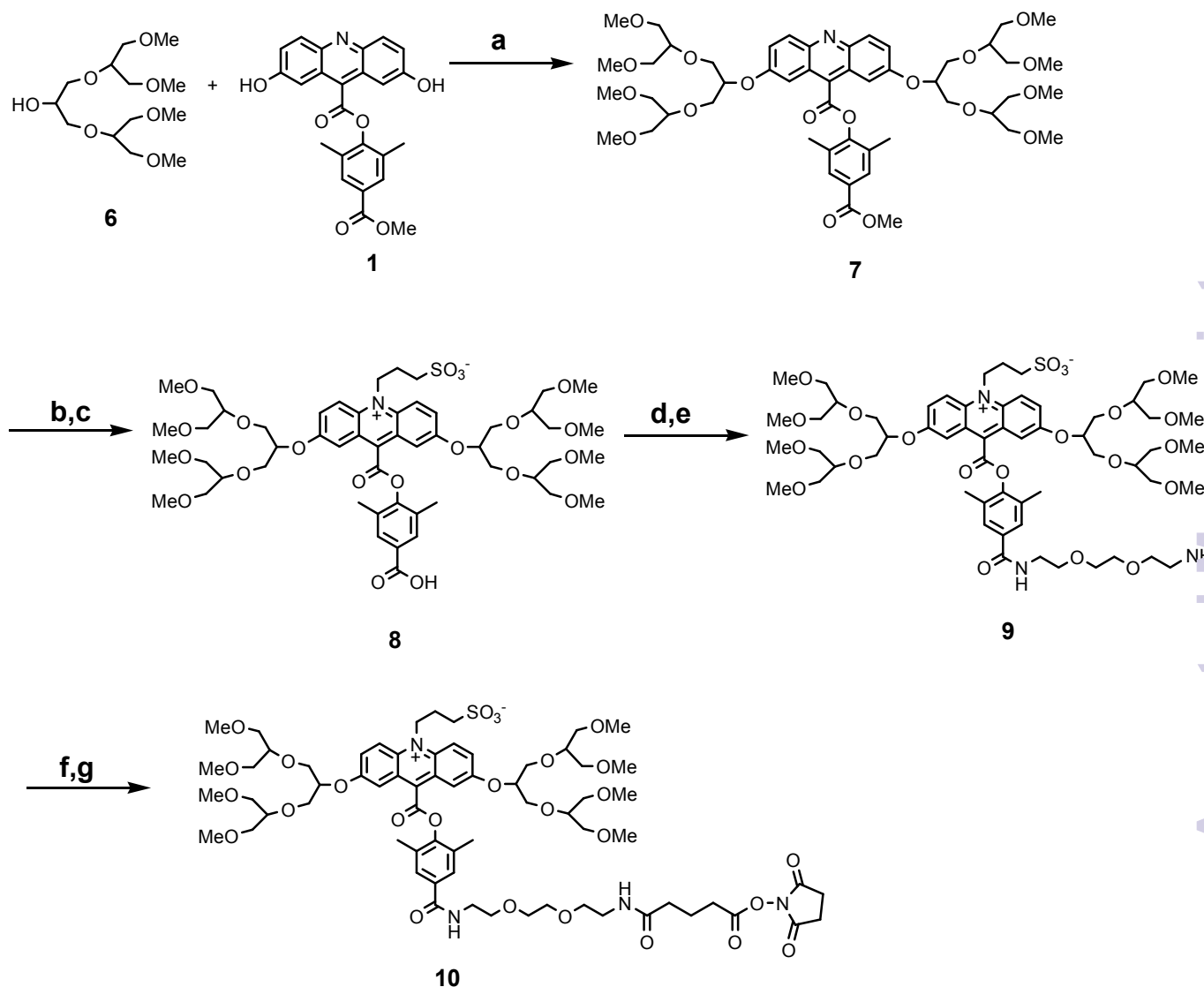


Figure 5. Synthetic scheme for compound **10**. Reagents : (a) triphenylphosphine (TPP), diisopropylazodicarboxylate (DIAD), triethylamine (TEA), tetrahydrofuran; (b) 1,3-propane sultone, 2,6-di-*tert*-butylpyridine, [BMIM][PF₆]; (c) 2M HCl; (d) TSTU, diisopropylethylamine DIPEA, DMF; (e) 2,2'-(ethylenedioxy)bis(ethylamine), DMF; (f) glutaric anhydride, DIPEA, DMF; (g) TSTU, DIPEA, DMF.

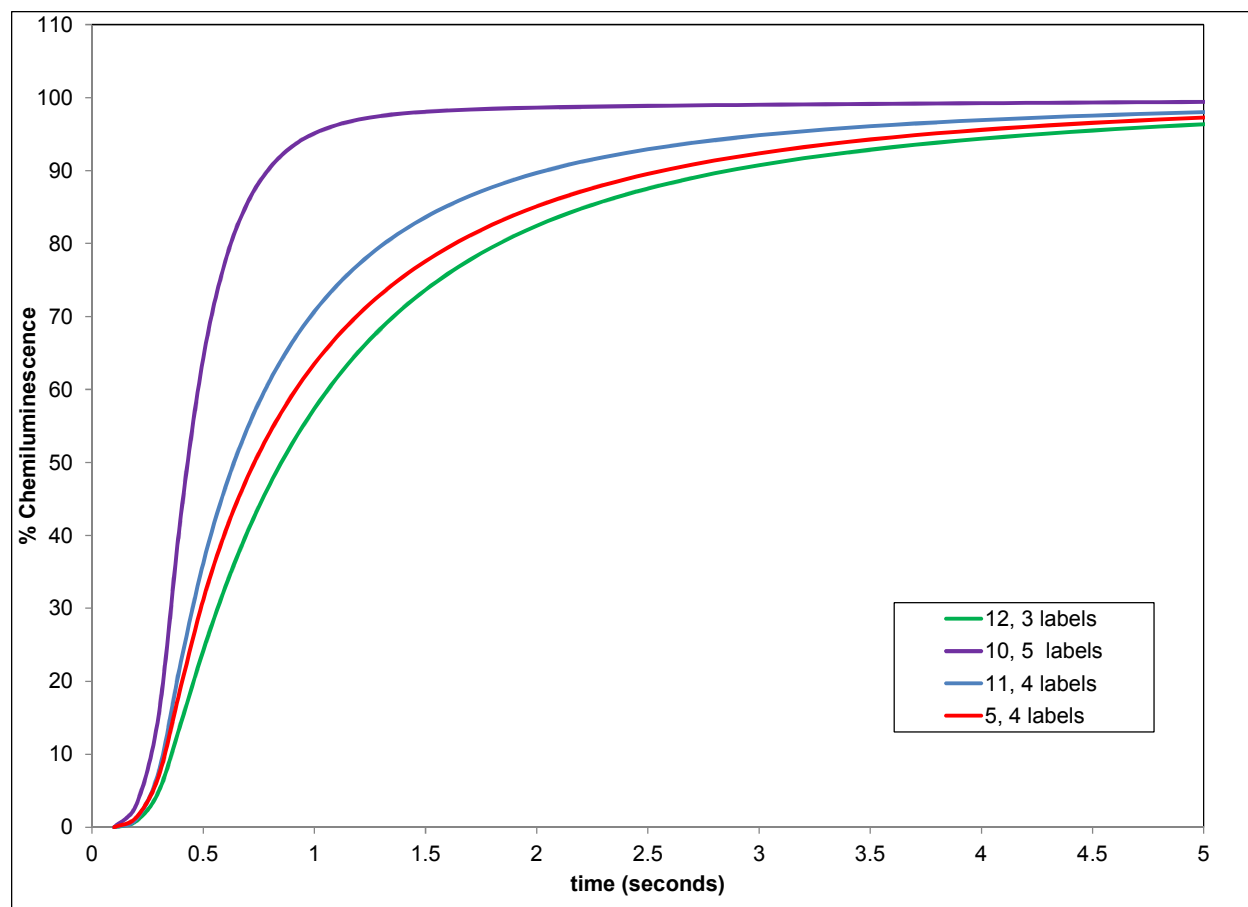


Figure 6. Kinetics of light emission of BSA conjugates of acridinium esters **5**, **10**, **11** and **12** in the presence of CTAC. Emission kinetics of the strongly anionic labels **5** and **11** were quite similar. On the other hand, emission from acridinium ester **10** with branched hexa(ethylene) glycol groups at C-2 and C-7 was rapid when compared to compound **12** with linear hexa(ethylene) glycol groups at C-2 and C-7 of the acridinium ring.

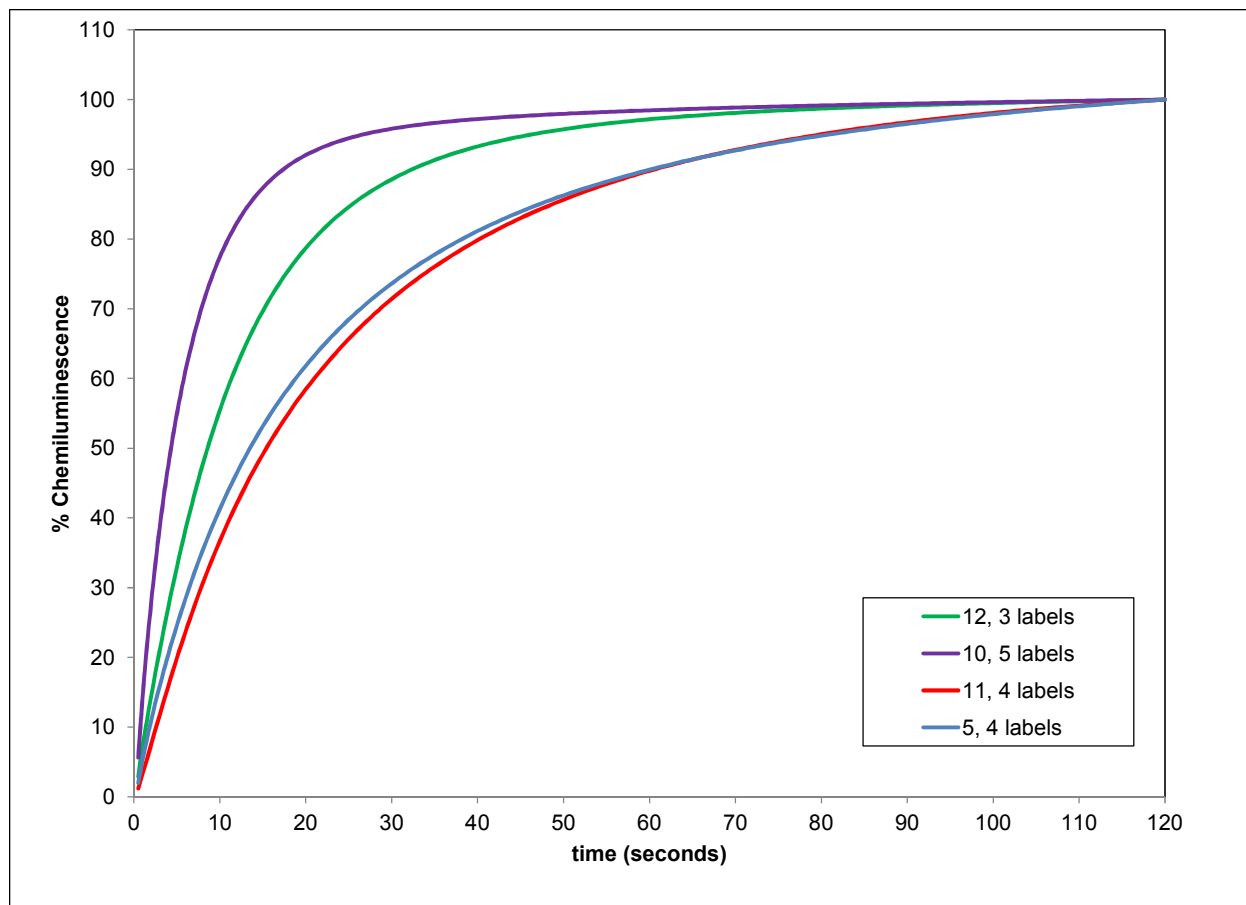


Figure 7. Kinetics of light emission of BSA conjugates of acridinium esters **5**, **10**, **11** and **12** in the absence of CTAC. Emission kinetics of the strongly anionic labels **5** and **11** were again quite similar to each other in the absence of surfactant. Emission from acridinium ester **10** with branched hexa(ethylene) glycol groups at C-2 and C-7 was faster when compared to compound **12** with linear hexa(ethylene) glycol groups are C-2 and C-7 of the acridinium ring.

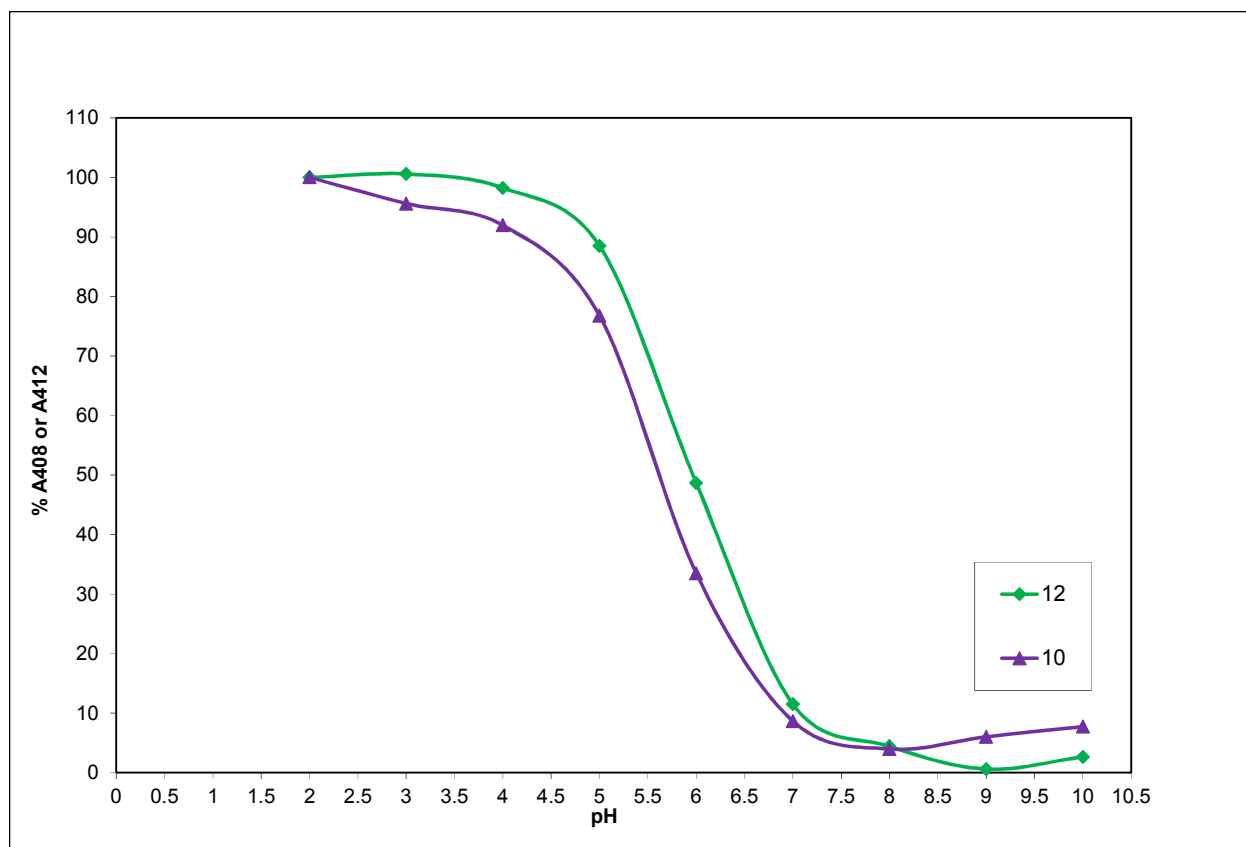


Figure 8. pH Titrations of compounds **10** and **12** illustrating conversion of the acridinium form **II** to the pseudobase **I** (refer to Figure 1). The branched hexa(ethylene) glycol groups in **10** induced a small shift in the pKa for pseudobase formation to acidic pH.

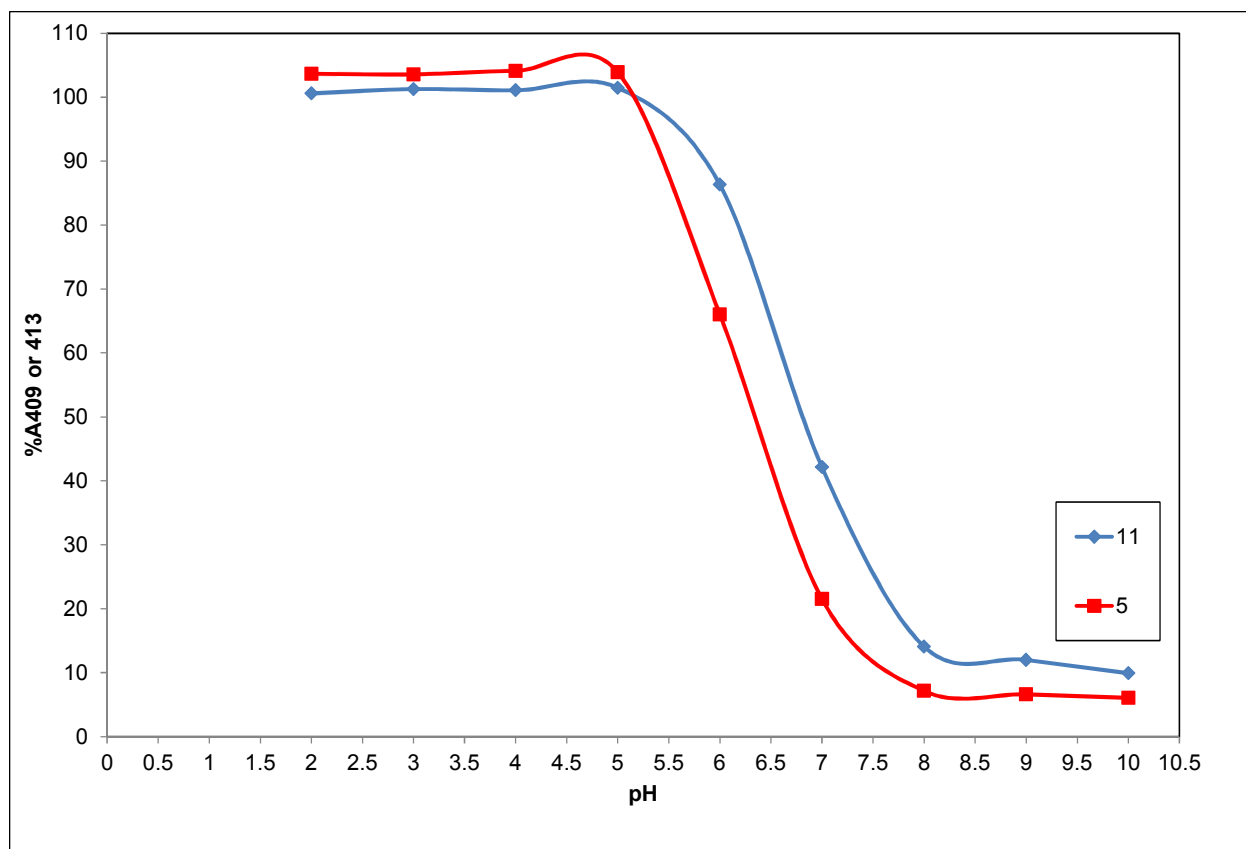


Figure 9. pH Titrations of compounds **11** and **5** illustrating conversion of the acridinium form **II** to the pseudobase **I**. Branching at the phenolic ethers in **5** induced a small shift in the pKa for pseudobase formation to acidic pH.

Table 1. Acridinium ester incorporation in BSA conjugates measured by mass spectroscopy, specific chemiluminescent activity (SCA) of the labels and time for $\geq 95\%$ emission. Light emission was triggered by the sequential addition of 0.3 mL reagent 1 (0.1 M nitric acid + 0.5% peroxide) followed by 0.3 mL reagent 2 (7 mM CTAC in 0.25 M NaOH). (RLU = Relative Light Unit). The strongly anionic labels **5** and **11** as well as the labels **10** with branched hexa(ethylene) glycol groups, and **12** with linear hexa(ethylene) glycol groups respectively all showed the same light yield because of the same C-2 and C-7 dialkoxy substitution pattern. Acridinium ester **10** showed the fastest emission time.

Label	No. of labels by mass spectroscopy	SCA x 10 ⁻¹⁹ RLU/mole	Time for $\geq 95\%$ emission (seconds)
5	4	6.1	3.8
10	5	4.6	1.2
11	4	4.3	3.0
12	3	5.3	5.3

Table 2. Residual chemiluminescence (% , average of five replicates) of BSA conjugates of the strongly anionic acridinium esters **5** and **11** as a function of pH at room temperature. Branching at the phenolic ethers in **5** improved long term stability at both pH 6 and pH 7.4. (CV = coefficient of variation of measurements).

Day	11 , pH = 6 (%CV)	5 , pH = 6 (%CV)	11 , pH = 7.4 (%CV)	5 , pH = 7.4 (%CV)
1	100 (2.5)	100 (2.7)	100 (2.2)	100 (3.8)
7	93 (2.3)	92 (4.6)	84 (2.7)	85 (2.4)
14	77 (3.8)	82 (3.3)	68 (2.5)	79 (4.4)
21	69 (3.1)	77 (2.8)	59 (4.2)	73 (4.7)
28	63 (3.9)	72 (3.2)	54 (4.1)	68 (1.0)
35	59 (3.2)	69 (2.6)	49 (2.2)	62 (2.2)

Table 3. Residual chemiluminescence (% , average of five replicates) of BSA conjugates of acridinium esters **10** and **12** as a function of pH at room temperature. Both acridinium esters with linear or branched hexa(ethylene) glycol groups at C-2 and C-7 exhibited similar stability. (CV = coefficient of variation of measurements).

Day	12 , pH = 6 (%CV)	10 , pH = 6 (%CV)	12 , pH = 7.4 (%CV)	10 , pH = 7.4 (%CV)
1	100 (4.9)	100 (5.8)	100 (7.2)	100 (2.0)
7	85 (3.8)	89 (7.7)	85 (3.5)	88 (3.3)
14	70 (3.3)	82 (4.3)	70 (2.6)	75 (4.4)
21	64 (3.3)	68 (3.6)	61 (3.5)	69 (5.9)
28	59 (3.2)	62 (4.3)	55 (3.4)	59 (3.6)
35	57 (1.5)	59 (5.7)	50 (4.4)	55 (3.7)